Rates of Direct Photolysis in Aquatic Environment

Richard G. Zepp* and David M. Cline

Environmental Research Laboratory, U.S. Environmental Protection Agency, College Station Road, Athens, Ga. 30601

■ Equations are derived that describe the direct photolysis rates of pollutants in the aquatic environment. The equations translate readily obtainable laboratory data into "half-lives" for photolysis under sunlight. Photolysis half-lives are calculated as a function of season, latitude, time-of-day, depth in water bodies, and ozone layer thickness. Experimental verification of the computed half-lives is presented.

The importance of photochemical transformation in the atmosphere is well-documented (*1, 2*), but comparatively little is known about photolysis of pollutants in water where other competing processes such as biodegradation and hydrolysis occur. A number of different photochemical processes may account for transformation of pollutants in the aquatic environment. One of these processes, direct photolysis, involves direct absorption of light by the pollutant followed by chemical reaction. Other photochemical processes may be initiated via light absorption by natural substances (indirect or "sensitized" photolysis) (*3–5*). In pure water or saturated hydrocarbons, direct photolysis is the only mechanism for photochemical transformation. During the past 10 years there has been a virtual explosion of interest in the photolysis of pollutants in solution, especially pesticides. Most of these studies have involved the identification of products derived from direct photolysis.

We have employed an approach that is quite useful in judging the likelihood that direct photolysis of a substance is or will be important in the aquatic environment (*6*). This approach involves utilization of a series of equations and laboratory data to compute direct photolysis rates under sunlight. The term "photolysis rate" as used in this paper refers to conversion per unit time, not to the very rapid rate of a primary photochemical process that deactivates a molecule in its electronically excited state. The relative importance of direct photolysis under a given set of environmental conditions can be assessed by comparison of the photolysis rate either with rates of competing processes or with what is known about the persistence of the substance under comparable field conditions (*6*). A similar approach described by Leighton (*2*) has been a valuable aid in disentangling the complexities of photochemical smog formation.

The rates of all photochemical processes in a water body are affected by solar spectral irradiance at the water surface, radiative transfer from air into water, and the transmission of sunlight in the water body. These subjects are briefly discussed below with references to more detailed reviews. Equations used to compute direct photolysis rates, results of the calculations, and experimental verification of the results are discussed in the balance of the paper.

Experimental

Computer Program. All computations were performed on a Digital Equipment Corp. PDP-8/E minicomputer. The computed results are either printed out or plotted on a Calcomp 563 plotter. Required data inputs are: (1) the molar extinction coefficients of the pollutant at wavelengths >297.5 nm (>285 nm for computation of the effects of ozone reduction); (2) the attenuation coefficients and refractive index of the reaction medium (attenuation coefficients for distilled water as reported by Hulbert and Dawson (*7, 8*) have already been incorporated into the program); (3) the quantum yield(s) for reaction of the pollutant; (4) the solar declination, solar right ascension, and sidereal time for the date of interest (obtained from the American Ephemeris and Nautical Almanac); (5) the latitude and longitude; and (6) the average ozone layer thickness, $\overline{X}$, that pertains to the season and location of interest [from London's compilations (*9*)].

To compute the relationship between solar altitude and time of day, a rearranged version of an equation described by Green and coworkers (*10*) was used. The rearranged version computes times of day (in universal time) as a function of solar altitude. Universal time is then converted to local time by the appropriate time zone correction.

For routine computations the program automatically inputs representative midseason data for items (4) and (6) above. Assumed midseason solar declinations are +10° for spring, +20° for summer, −10° for fall, and −20° for winter. The program then computes midseason photolysis rate constants and half-lives as a function of local time of day for a given longitude and for any specified combination of depth, season, and latitude (ranging from 0° to 90°N in 10° increments).

Another subroutine in the program computes representative effects of variation in ozone layer thickness upon photolysis rates for three latitudes, 0°, 40°, and 73°N.

Solar Radiation Data. All values for intensity of ultraviolet radiation (297.5–380 nm) were derived from a report published by Bener (*11*). Sky intensity $H(\lambda, ho, \overline{X})$ was computed according to an empirical relation described by Bener (Equation 1)

$$\log H(\lambda, ho, \overline{X}) = \log H(\lambda, ho, Xo) - T(\lambda, ho)(\overline{X} - Xo) \quad (1)$$

where $H(\lambda, ho, Xo)$ is the sky intensity at solar altitude ho, wavelength λ, and a reference ozone value, Xo, and $T(\lambda, ho)$ is a coefficient. Parameters for each wavelength and solar altitude were computed from the extensive data in Bener's report. A similar equation was used to obtain the values of direct solar intensity as a function of ozone layer thickness. These data were converted from W cm^{-2} nm^{-1} to photons cm^{-2} s^{-1} nm^{-1} by Equation 2 where λ is the wavelength in nm.

$$I(\text{photons cm}^{-2}\,\text{s}^{-1}\,\text{nm}^{-1}) = I(\text{W cm}^{-2}\,\text{nm}^{-1}) \times \lambda \times 5.035 \times 10^{15} \quad (2)$$

Approximate intensity values for visible solar radiation (390–800 nm) were calculated by computer using equations described by Leighton (*2*). Data used in these computations were derived from the following sources.

- Values for extraterrestrial solar irradiance were taken from Johnson's data (*12*).
- Atmospheric transmissivity with respect to scattering was computed using equations in Leighton's book (*2*).
- Absorption coefficients for ozone were obtained from a paper by Inn and Tanaka (*13*).

Experimental Procedures. The procedures and equipment used to measure the quantum yields for reaction have been discussed previously (*6*). All quantum yields used in the computations pertain to air-saturated water, hexane, or hexadecane. Electronic absorption spectra were obtained on Perkin-Elmer 602 or Perkin-Elmer 356 spectrophotometers. Since it was impossible to measure the spectra of highly water-insoluble compounds in water, the spectra were measured in water–acetonitrile.

Dilute solutions were exposed to sunlight in 1-cm-deep uncovered culture dishes that were filled to the brim and in stoppered quartz cells that were horizontal to the ground. The detailed studies with 1,1-bis(*p*-methoxyphenyl)-2,2-dichloroethylene (DMDE) were conducted in dishes using hexadecane as solvent. For those compounds that volatilized rapidly from the water, such as trifluralin, sunlight photolyses were conducted in the stoppered cells. The photolysis rates in the quartz cells were more rapid than those observed in the dishes, since internal reflection of sunlight in the cells increased the pathlength of the light. To correct for this effect, midday photolysis rates measured in the cells were multiplied by a factor that equaled the ratio of the midday photolysis rate of the pollutant in the dish to that in the cell, using hexadecane as solvent. In all cases discussed in this paper, no change in concentration occurred in dark controls during the period of sunlight exposure.

Results and Discussion

Solar Radiation at the Earth's Surface. Photolysis rates are strongly influenced by the intensity and spectral distribution of the light source. Detailed discussions of the nature of sunlight at the earth's surface appear elsewhere (*2, 10–11, 14–16*). Some highlights of these discussions that are pertinent to this paper are summarized below.

As sunlight passes through the atmosphere, its intensity is decreased through absorption by atmospheric gases, such as ozone, and by molecular and aerosol scattering. The transmittance of the atmosphere in the ultraviolet and visible region decreases with decreasing wavelength; essentially no light is transmitted at wavelengths <295 nm. The sharp decrease in intensity in the 280–320-nm region is due mainly to ozone absorption. This part of sunlight, often called UV-B radiation, causes sunburn and other biologic effects and is responsible for direct photolysis of many pollutants, including most commonly used pesticides.

The intensity and spectral distribution of sunlight on a horizontal surface change constantly. Generally, the intensity decreases with decreasing angular height of the sun. Thus, intensity decreases from midday to sunset, from summer to winter, and from the tropics to higher latitudes.

The decrease in UV-B intensity with decreasing solar altitudes is much more pronounced than the decrease in visible or UV-A (320–400 nm) intensity. The intensity of UV-B radiation is also strongly influenced by seasonal and geographic variations in atmospheric ozone amount. Increases in ozone amount occur with increasing northern latitude and from fall (minimum) to spring (maximum) (*9*). The intensity values used in the computations discussed below are based upon *average* ozone amounts at various latitudes and seasons as compiled by London (*9*). Deviations from the averages are discussed elsewhere (*9, 16*).

Atmospheric scattering increases with decreasing wavelength and is most pronounced in the blue and ultraviolet region. Scattered light illuminates the sky causing its blue appearance. The fraction of light from the sky exceeds 50% in the UV-B region. Thus, solar radiation at a given spot on the earth's surface is derived both directly from the sun and also from the sky.

Radiative Transfer from the Atmosphere into a Water Body. When a beam of sunlight encounters the surface of a water body, part is reflected at an angle equal to the angle of incidence, z, and part passes into the water body with a change in direction due to refraction (Figure 1). The fraction of direct sunlight that is reflected, RFD, can be computed by Fresnel's law and is less than 10% at all but very large values of z. Assuming the sky is uniformly bright, we computed that the reflected fraction of sky radiation, RFS, is about 0.07 (*17*). The values of RFD and RFS that were used in our calculations (Table I) were computed assuming that the refractive index, n, of water is 1.34, a value that pertains specifically to blue light (436 nm). Since the refractive index increases slightly with decreasing wavelength (*18*), the computed reflectivities are somewhat higher for ultraviolet light and somewhat lower for long wavelength visible light. The computed values agree closely with experimental data obtained from studies of natural water bodies (*19*).

Pathlengths of Sunlight in Water Bodies. The pathlength is defined as the distance traveled by a beam of sunlight as it passes through a horizontal layer of the atmosphere or a water body. Pathlengths of direct and sky radiation are used in equations that compute photolysis rates (see next section). In the atmosphere the pathlength of direct radiation is h sec z where h is the thickness of a horizontal layer (Figure 1). Underwater, the light is bent downward and assumes a pathlength, l_d, of D sec θ where D is the depth and θ is the angle of refraction. The relationship between the angles z and

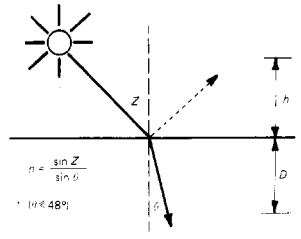

Figure 1. Diagram of passage of beam of sunlight through atmosphere into water body
Z = angle of incidence (solar zenith angle in case of direct sunlight); θ = angle of refraction

Table I. Intensities and Pathlengths of Solar Radiation in Atmosphere and Water Bodies

	Atmosphere[a]	Water body
Direct intensity on horizontal plane	$S \cos z$	$S \cos z\,(1\text{-RFD}) = I_d$
Sky intensity on horizontal plane	H	$H\,(1\text{-RFS}) = I_s$
Pathlength of direct radiation	$h \sec z$	$D \sec \theta = l_d$
Average pathlength of sky radiation	$2h$	$1.2\,D = l_s$

[a] Ref. *2*.

θ is defined by Snell's law (Figure 1). As the solar zenith angle, z, increases, so does the amount of refraction. Light coming from the horizon ($z > 85°$) is strongly bent, assuming an underwater angle, θ, of 48°.

Leighton has shown that the average pathlength for sky radiation in the atmosphere is close to $2h$ (*2*). Neglecting reflection and assuming that the sky is uniformly bright, it can be shown that the average pathlength for sky radiation underwater can be expressed by Equation 3 (*17*):

$$l_s = 2Dn\,(n - \sqrt{n^2 - 1}) \tag{3}$$

Assuming n is 1.34, the computed pathlength is $1.20D$. Taking reflection into account, the computed pathlength is $1.19D$ (*17*). Reflection has little effect on the computed value, because the most strongly reflected part of sky radiation (near horizon) contributes only a small fraction of the total sky intensity on a horizontal plane (*2*). Other workers have computed similar values for the underwater pathlength of sky radiation (*20–22*). Results discussed in this and the preceding section are summarized in Table I.

Light Attenuation in Natural Waters. As in the atmosphere, the intensity of sunlight is attenuated in natural waters through absorption and scattering (*23*). In the ocean, absorption is primarily due to water itself (*24*). Because water is most transparent in the blue region and scattering is relatively wavelength-independent, solar radiation in clear ocean water assumes a blue hue at great depths (*24*). Sunlight penetrates much more deeply into the ocean than into inland surface waters (*19*) where absorption is due mainly to dissolved natural organics (*24*). The attenuation coefficients, α_λ, that we measured for inland surface waters in the ultraviolet region are wavelength-dependent and can vary considerably from one water body to another (Figure 2). In Figure 2, $2/\alpha$ is the distance in which 99% of the incident intensity of a collimated beam of light is attenuated in passing through the water. Even in the relatively clear waters of the Savannah River, the attenuation coefficients are higher than those reported for distilled water in the ultraviolet region (*8*). Average attenuation coefficients for 10 river water samples collected in the Southeastern United States are shown in Figure 3. The average data should not be regarded as typical; variations were about ±95% in the UV-B region. Nonetheless, the general shape of the attenuation curve is representative. Attenuation of light intensity generally increases with decreasing wavelength in the visible and ultraviolet region.

Attenuation due to light scattering is less important than attenuation by absorption in most natural waters especially in the ultraviolet region (*16, 19, 23–24*). As a first approximation, scattering was ignored in the following considerations.

Equations Describing Direct Photolysis (25). Scientists realized long ago that only light which is absorbed can effect chemical change in a system. This basic law of photochemistry was first enunciated by Grotthus and then Draper in the nineteenth century. The average photolysis rate, $(-d[P]/dt)_\lambda$, at a certain wavelength λ in a completely mixed water body is directly proportional to the rate of light absorption by the pollutant per unit volume. The amount of light absorbed per unit time, I_λ, is defined by Lambert's law (Equation 4) where α_λ is the decadic absorption coefficient of the water body, l is the pathlength of the light, and I_o is the incident light intensity.

$$I_\lambda = I_{o\lambda}\,(1 - 10^{-\alpha_\lambda l}) \tag{4}$$

The average rate of absorption per unit volume, $I_{a\lambda}$, for underwater solar radiation in a layer of depth D is

$$I_{a\lambda} = \frac{I_{d\lambda}(1 - 10^{-\alpha_\lambda l_d}) + I_{s\lambda}(1 - 10^{-\alpha_\lambda l_s})}{D} \tag{5}$$

The pathlengths l_d and l_s can be computed as described above.

The addition of a pollutant to the water body changes its absorption coefficient to $(\alpha_\lambda + \epsilon_\lambda[P])$ where ϵ_λ is the molar extinction coefficient of the pollutant, and $[P]$ is its concentration. The fraction of light that is absorbed by the pollutant is $\epsilon_\lambda[P]/(\alpha_\lambda + \epsilon_\lambda[P])$. Since pollutant concentrations in water bodies are usually very low, $\epsilon_\lambda[P]$ is usually much smaller than α_λ, and $(\alpha_\lambda + \epsilon_\lambda[P]) \cong \alpha_\lambda$. Thus, the average rate of light absorption by a pollutant, $I'_{a\lambda}$, may be expressed as

$$I'_{a\lambda} = I_{a\lambda}\frac{\epsilon_\lambda[P]}{j\alpha_\lambda} \tag{6}$$

$$I'_{a\lambda} = k_{a\lambda}[P] \tag{7}$$

where $k_{a\lambda} = I_{a\lambda}\epsilon_\lambda/j\alpha_\lambda$ and j is a constant that converts the intensity units into units that are compatible with $[P]$ (j equals 6.02×10^{20} when $[P]$ is expressed in moles/liter and intensity is expressed in photons $cm^{-2}\ s^{-1}$).

The equation for $k_{a\lambda}$ simplifies under two circumstances:

- If $\alpha_\lambda l_d$ and $\alpha_\lambda l_s$ are both greater than 2, then essentially all the sunlight responsible for photolysis is absorbed by the system and the expression for $k_{a\lambda}$ becomes

$$k_{a\lambda} = \frac{W_\lambda \epsilon_\lambda}{jD\alpha_\lambda} \tag{8}$$

where W_λ equals $(I_{d\lambda} + I_{s\lambda})$. Values of W_λ for midday and midseason at latitude 40°N are summarized in Table II. This equation shows that at depths greater than that of the photic zone, the average photolysis rate is inversely proportional to depth.

- If $\alpha_\lambda l_d$ and $\alpha_\lambda l_s$ are both less than 0.02, then $k_{a\lambda}$ becomes independent of α_λ and can be approximately expressed as:

$$k_{a\lambda} = \frac{2.303\,\epsilon_\lambda(I_{d\lambda}l_d + I_{s\lambda}l_s)}{jD} \tag{9}$$

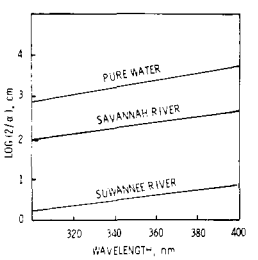

Figure 2. Attenuation of ultraviolet light in pure water and in water obtained from two rivers

$2/\alpha$ is distance corresponding to 99% attenuation of incident intensity of beam of light traveling through water

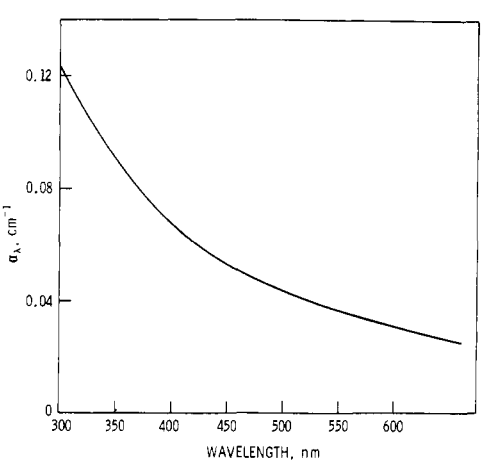

Figure 3. Average attenuation coefficients for 10 river water samples collected in southeastern U.S.

Table II. W_λ and Z_λ Values for Latitude 40°N

Wavelength (nm)	Spring	Summer	Fall	Winter
		W_λ values		
		Photons (cm^{-2} s^{-1} 2.5 nm^{-1})		
297.5	0.240E + 12	0.648E + 12	0.786E + 11	0.000E + 00
300.0	0.105E + 13	0.219E + 13	0.434E + 12	0.601E + 11
302.5	0.369E + 13	0.657E + 13	0.185E + 13	0.300E + 12
305.0	0.106E + 14	0.163E + 14	0.555E + 13	0.139E + 13
307.5	0.195E + 14	0.274E + 14	0.112E + 14	0.369E + 13
310.0	0.325E + 14	0.444E + 14	0.173E + 14	0.698E + 13
312.5	0.510E + 14	0.643E + 14	0.308E + 14	0.145E + 14
315.0	0.683E + 14	0.836E + 14	0.410E + 14	0.222E + 14
317.5	0.867E + 14	0.103E + 15	0.532E + 14	0.296E + 14
320.0	0.103E + 15	0.121E + 15	0.663E + 14	0.408E + 14
		Photons (cm^{-2} s^{-1} 3.75 nm^{-1})		
323.1	0.193E + 15	0.226E + 15	0.119E + 15	0.740E + 14
		Photons (cm^{-2} s^{-1} 10 nm^{-1})		
330.0	0.669E + 15	0.762E + 15	0.421E + 15	0.279E + 15
340.0	0.778E + 15	0.875E + 15	0.500E + 15	0.341E + 15
350.0	0.835E + 15	0.938E + 15	0.533E + 15	0.363E + 15
360.0	0.895E + 15	0.100E + 16	0.568E + 15	0.383E + 15
370.0	0.997E + 15	0.112E + 16	0.623E + 15	0.418E + 15
380.0	0.110E + 16	0.124E + 16	0.679E + 15	0.450E + 15
390.0	0.133E + 16	0.148E + 16	0.895E + 15	0.646E + 15
400.0	0.191E + 16	0.212E + 16	0.129E + 16	0.931E + 15
410.0	0.251E + 16	0.279E + 16	0.170E + 16	0.123E + 16
420.0	0.258E + 16	0.287E + 16	0.175E + 16	0.127E + 16
430.0	0.249E + 16	0.277E + 16	0.170E + 16	0.123E + 16
440.0	0.295E + 16	0.327E + 16	0.201E + 16	0.146E + 16
450.0	0.332E + 16	0.368E + 16	0.227E + 16	0.164E + 16
460.0	0.335E + 16	0.372E + 16	0.230E + 16	0.167E + 16
470.0	0.347E + 16	0.384E + 16	0.238E + 16	0.172E + 16
480.0	0.355E + 16	0.394E + 16	0.244E + 16	0.177E + 16
490.0	0.336E + 16	0.372E + 16	0.231E + 16	0.168E + 16
500.0	0.343E + 16	0.380E + 16	0.236E + 16	0.171E + 16
525.0	0.362E + 16	0.401E + 16	0.251E + 16	0.181E + 16
550.0	0.377E + 16	0.418E + 16	0.262E + 16	0.188E + 16
575.0	0.380E + 16	0.423E + 16	0.265E + 16	0.190E + 16
600.0	0.385E + 16	0.427E + 16	0.268E + 16	0.192E + 16
625.0	0.387E + 16	0.428E + 16	0.271E + 16	0.196E + 16
650.0	0.389E + 16	0.429E + 16	0.273E + 16	0.199E + 16
675.0	0.388E + 16	0.427E + 16	0.273E + 16	0.200E + 16
700.0	0.384E + 16	0.422E + 16	0.272E + 16	0.200E + 16
750.0	0.369E + 16	0.404E + 16	0.261E + 16	0.193E + 16
800.0	0.354E + 16	0.387E + 16	0.252E + 16	0.187E + 16
		Z_λ values		
		Photons (cm^{-2} s^{-1} 2.5 nm^{-1})		
297.5	0.274E + 12	0.716E + 12	0.949E + 11	0.000E + 00
300.0	0.120E + 13	0.240E + 13	0.524E + 12	0.733E + 11
302.5	0.419E + 13	0.723E + 13	0.223E + 13	0.368E + 12
305.0	0.121E + 14	0.181E + 14	0.670E + 13	0.170E + 13
307.5	0.223E + 14	0.305E + 14	0.135E + 14	0.450E + 13
310.0	0.372E + 14	0.495E + 14	0.208E + 14	0.854E + 13
312.5	0.584E + 14	0.717E + 14	0.371E + 14	0.177E + 14
315.0	0.780E + 14	0.933E + 14	0.494E + 14	0.271E + 14
317.5	0.992E + 14	0.115E + 15	0.641E + 14	0.362E + 14
320.0	0.117E + 15	0.135E + 15	0.800E + 14	0.498E + 14
		Photons (cm^{-2} s^{-1} 3.75 nm^{-1})		
323.1	0.221E + 15	0.252E + 15	0.144E + 15	0.906E + 14
		Photons (cm^{-2} s^{-1} 10 nm^{-1})		
330.0	0.761E + 15	0.846E + 15	0.508E + 15	0.342E + 15
340.0	0.880E + 15	0.963E + 15	0.604E + 15	0.420E + 15
350.0	0.942E + 15	0.103E + 16	0.645E + 15	0.449E + 15
360.0	0.101E + 16	0.110E + 16	0.687E + 15	0.479E + 15
370.0	0.112E + 16	0.122E + 16	0.754E + 15	0.520E + 15
380.0	0.124E + 16	0.135E + 16	0.822E + 15	0.562E + 15
390.0	0.149E + 16	0.161E + 16	0.108E + 16	0.805E + 15
400.0	0.213E + 16	0.231E + 16	0.156E + 16	0.116E + 16
410.0	0.280E + 16	0.302E + 16	0.206E + 16	0.154E + 16
420.0	0.288E + 16	0.310E + 16	0.212E + 16	0.159E + 16
430.0	0.277E + 16	0.298E + 16	0.205E + 16	0.154E + 16
440.0	0.327E + 16	0.351E + 16	0.244E + 16	0.184E + 16
450.0	0.368E + 16	0.394E + 16	0.275E + 16	0.208E + 16

Table II. Continued

Wavelength (nm)	Spring	Summer	Fall	Winter
		Photons (cm^{-2} s^{-1} 10 nm^{-1})		
460.0	0.371E + 16	0.398E + 16	0.279E + 16	0.211E + 16
470.0	0.384E + 16	0.411E + 16	0.289E + 16	0.219E + 16
480.0	0.392E + 16	0.420E + 16	0.296E + 16	0.225E + 16
490.0	0.371E + 16	0.396E + 16	0.281E + 16	0.213E + 16
500.0	0.378E + 16	0.404E + 16	0.287E + 16	0.218E + 16
525.0	0.398E + 16	0.426E + 16	0.305E + 16	0.232E + 16
550.0	0.413E + 16	0.442E + 16	0.318E + 16	0.241E + 16
575.0	0.417E + 16	0.446E + 16	0.322E + 16	0.243E + 16
600.0	0.421E + 16	0.450E + 16	0.326E + 16	0.247E + 16
625.0	0.422E + 16	0.450E + 16	0.329E + 16	0.252E + 16
650.0	0.424E + 16	0.451E + 16	0.332E + 16	0.256E + 16
675.0	0.423E + 16	0.448E + 16	0.333E + 16	0.259E + 16
700.0	0.419E + 16	0.443E + 16	0.330E + 16	0.258E + 16
750.0	0.401E + 16	0.423E + 16	0.318E + 16	0.250E + 16
800.0	0.385E + 16	0.405E + 16	0.306E + 16	0.242E + 16

Equation 9 applies even if $\epsilon_\lambda[P]$ exceeds α_λ as long as (α_λ + $\epsilon_\lambda[P]$) is less than 0.02; i.e., less than 5% of the light is absorbed by the system. By substituting the equations defining pathlengths l_d and l_s (Table I) into Equation 9, Equation 10 is obtained:

$$k_{a\lambda} = 2.303\ \epsilon_\lambda{}^{j-1} Z_\lambda \tag{10}$$

where

$$Z_\lambda = I_{d\lambda} \sec\theta + 1.2\, I_{s\lambda} \tag{11}$$

This equation is approximately applicable to shallow depths in any natural water and depths up to one-half meter in distilled water. Midday, midseason values of Z_λ for latitude 40°N are presented in Table II.

The values shown in Table II correspond to wavelength intervals centered at the specified wavelength. For example, the Z_λ value for 350 nm corresponds to the 10-nm interval from 345 to 355 nm. Extinction coefficients, ϵ_λ, used in calculations are averaged over the wavelength intervals that correspond to those in the table.

The second law of photochemistry, the Stark-Einstein law, states that one molecule is activated for each light quantum or photon absorbed in a system. Thus, photolysis rates are proportional to the total number of photons absorbed per unit time, not the total energy absorbed. After a molecule absorbs a photon, it is unstable and will undergo a variety of competing *primary processes*, such as chemical reaction, light emission, or physical deactivation, to return to a stable state. The fraction of photons absorbed that results in a certain primary process is called the *primary quantum yield*, Φ, for the process. A corollary of the Stark-Einstein law is that the sum of the primary quantum yields of all the processes that deactivate an excited molecule equals unity. The primary quantum yield of a photochemical process in solution sometimes differs from the experimentally measured quantum yield for reaction, ϕ. For example, secondary thermal reactions such as free radical chain reactions can cause the value of ϕ to exceed unity, or reversal of a photochemical cleavage can cause the observed quantum yield to be much lower than the primary quantum yield. It is unlikely that chain reactions initiated by direct photolysis of a pollutant are important at the very low concentrations of pollutants that are found in lakes and rivers. Most inland waters contain phenolic humic materials, and phenols inhibit chain reactions. Thus, quantum yields for direct photolysis in the aquatic environment are not likely to exceed unity. More detailed discussions of quantum yields and their measurement appear elsewhere (*26*, *27*).

The average photolysis rate is also proportional to the quantum yield for reaction, ϕ. The kinetic expression for direct photolysis is

$$-\left(\frac{d[P]}{dt}\right)_\lambda = \phi_\lambda k_{a\lambda}[P] \tag{12}$$

The quantum yield for reaction of complex molecules in solution is usually not wavelength-dependent (*28*). Accordingly, the complete rate expression is

$$-\frac{d[P]}{dt} = \phi k_a[P] \tag{13}$$

where k_a equals $\Sigma k_{a\lambda}$, the sum of the $k_{a\lambda}$ values for all wavelengths of sunlight that are absorbed by the pollutant. This expression has the form of a first-order rate equation in which the photolysis rate constant, ϕk_a, is expressed in units of reciprocal time. The concentration-independent half-life, $t_{1/2}$, inherent to direct photolysis is

$$t_{1/2} = \frac{0.693}{\phi k_a} \tag{14}$$

Since the value of ϕ is not likely to exceed unity, it follows that

$$t_{1/2} \leq \frac{0.693}{k_a} \tag{15}$$

Some sunlight photolysis rates reported in the literature have been measured under experimental conditions in which the pollutant absorbs much more light than the solvent, i.e., $\Sigma\epsilon_\lambda[P] \gg \Sigma\alpha_\lambda$. Under these conditions, if *all* the incident light is absorbed, the photolysis kinetics become zero order, and the half-life (Equation 16) becomes dependent on the initial pollutant concentration, $[P_o]$, and depth, D.

$$t_{1/2} = \frac{jD[P_o]}{2\,\phi\Sigma W_\lambda} \tag{16}$$

Thus, half-lives measured at high pollutant concentrations can be much longer than those observed at concentrations similar to those found in the aquatic environment.

Results of Calculations. We have developed a computer program written in Fortran IV that uses the above-mentioned equations and intensities of solar radiation to compute direct photolysis rates. The program, which is available on request, will be described in more detail elsewhere.

To illustrate the results of the calculations, photolysis rates were computed for carbaryl, a widely used carbamate insecticide, and trifluralin, a popular preemergent herbicide.

Carbaryl, a naphthalene derivative, absorbs UV-B radiation most strongly, and trifluralin, a dinitroaniline derivative, absorbs sunlight strongly in the visible region (Figure 4). The $k_{a\lambda}$ values shown in Figure 4 were computed for a shallow depth (see Equation 9) and apply to midsummer and midday at latitude 40°N. The quantum yields for reaction of carbaryl and trifluralin in air-saturated water are similar, 0.006 (313 nm) and 0.002 (366 nm), respectively (*29*). However, the sunlight absorption rate of trifluralin is about 400 times larger. Consequently, direct photolysis of trifluralin is over two orders of magnitude more rapid than photolysis of carbaryl.

The computed midday photolysis half-lives (near-surface) of the two pesticides depend upon season and latitude (Figure 5). The results in Figure 5 were computed as relative values, where the half-life of each pesticide for midsummer at latitude 30°N was assigned a value of unity. Seasonal variations occur for both pesticides at the midlatitudes with minimum half-lives occurring during summer, the period of maximum pesticide use, and maximum values occurring during winter. Both the half-lives and the amplitude of their seasonal variation increase with increasing northern latitude. In the tropical zone, photolysis rates are approximately constant throughout the year. However, in the midlatitudes the amplitudes of seasonal variation are much larger for carbaryl than for trifluralin. Latitudinal variation is relatively small during the summer. The seasonal variations shown for carbaryl are similar to those computed for most commonly used pesticides.

As the intensity of sunlight increases and then decreases throughout the day, so do the photolysis rates (Figure 6). The computed rates in Figure 6 are relative to photolysis rates at midday and midsummer and apply to shallow depths only. Because UV-B "sunrise" and "sunset" lags and precedes, respectively, visible sunrise and sunset, the period of photolysis for carbaryl is shorter than that for trifluralin. In comparing photolysis rates with rates of other processes such as hydrolysis or volatilization, the photolysis rates are integrated over the entire period of a day (*6*).

As sunlight passes down through a water body, its intensity decreases, and marked changes in its spectral distribution occur. The decrease in photolysis rate with increasing depth depends upon the magnitude and spectral distribution of: the attenuation coefficients of the water body, the molar extinction coefficients of the pollutant, and the intensity values of sunlight. The computed depth dependence of the direct photolysis of carbaryl and trifluralin at midday and midsummer (latitude 40°N) is shown in Figure 7. Results were calculated using attenuation coefficients of pure water and "average river water" shown in Figures 2 and 3. The photolysis rates of both pesticides drop off much more rapidly in the river water than in pure water. In lake or ocean water, the depth dependence is usually similar to that shown for pure water. Since UV-B radiation is absorbed more strongly than visible light in both pure and river water, the photolysis rate of carbaryl decreases more rapidly with increasing depth than that of trifluralin. Note, however, that the rate of decrease with increasing depth becomes identical for both pesticides once the depth corresponding to the photic zone is exceeded (see Equation 8). The underwater pathlength of direct sunlight lengthens, and depth dependence increases as the sun moves lower in the sky. Consequently, the depth dependence becomes more pronounced with increasing northern latitude (*6*) and from summer to winter in the midlatitudes.

All of the above computations for carbaryl were based upon average UV-B intensities for each season and latitude circle. Natural variations in the ozone layer (*9, 16*) can cause significant deviations from the average intensity values. Moreover, there is growing evidence that certain anthropogenic activities may lead to a depletion of the ozone layer (*30*). The effect of

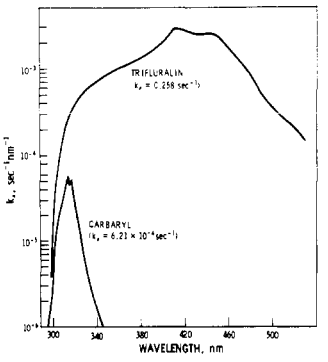

Figure 4. Specific sunlight absorption rates of carbaryl and trifluralin as function of wavelength at midday and midsummer, latitude 40°N

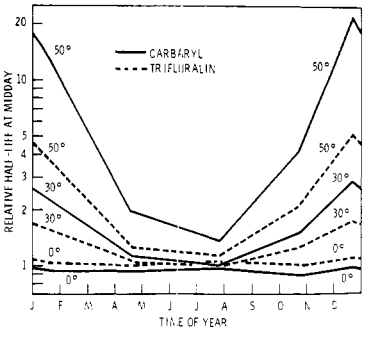

Figure 5. Relative midday half-lives for direct photolysis of carbaryl and trifluralin at midseason for several northern latitudes

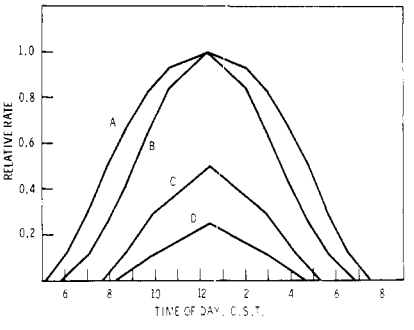

Figure 6. Diurnal variation of direct photolysis rates of trifluralin and carbaryl at latitude 40°N, longitude 90°W

A, trifluralin, 7/24/75; B, carbaryl, 7/24/75; C, trifluralin, 1/21/75; D, carbaryl, 1/21/75

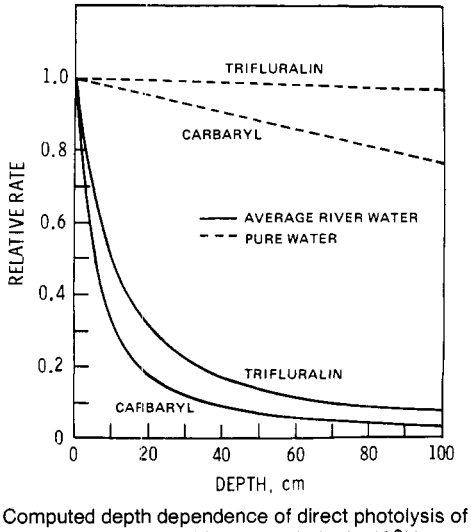

Figure 7. Computed depth dependence of direct photolysis of carbaryl and trifluralin at midday and midsummer, latitude 40°N

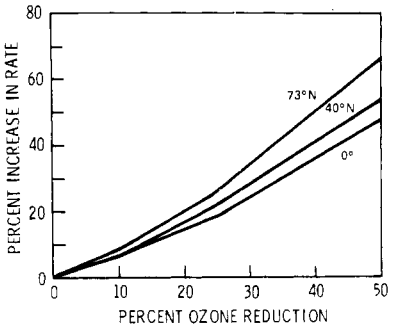

Figure 8. Effect of ozone reduction upon direct photolysis of carbaryl at selected northern latitudes

Ozone thickness assumed for zero reduction: lat 0°, 0.248 cm; lat 40°N, 0.319 cm; lat 73°N, 0.366 cm. Solar altitudes assumed: lat 0° and 40°N, 60°; lat 73°N, 40°

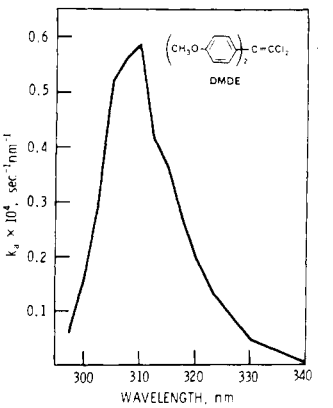

Figure 9. Absorption of solar radiation by 1,1-bis(*p*-methoxyphenyl)-2,2-dichloroethylene (DMDE) at midday, midsummer, latitude 40°N

ozone reduction upon the photolysis rates of carbaryl at three latitudes is shown in Figure 8. The photolysis rate of trifluralin is essentially unaffected by ozone variation because ozone is transparent to wavelengths of sunlight that are strongly absorbed by trifluralin.

Experimental Verification. Studies by Hedlund and Youngson (*31*) of the photolysis of the pesticide, picloram, under sunlight have verified that:

- Photolysis in dilute solution obeys a first-order rate expression (Equation 13). Thus, the photolysis half-life is concentration-independent in dilute solution.
- The photolysis half-life increases with increasing depth.
- At shallow depths, direct photolysis rates are the same regardless of the nature of the water, be it distilled or of natural origin (Equation 9).

To check the results of our calculations, we have determined the photolysis rates of several pesticides and organomercury compounds (*32*) at shallow depths under sunlight in Athens, Ga. (latitude 34°N). The direct photolysis of DMDE (*33*) was examined in some detail. DMDE was chosen because it photodegrades very rapidly under sunlight and, like most pesticides, absorbs UV-B radiation most strongly (Figure 9). Dilute solutions of DMDE (1.00×10^{-7} M) in uncovered dishes were exposed to sunlight for 1–1.5 h at different times of the day in an open field. The solutions were analyzed, and average photolysis rate constants (ϕk_a values) were computed for each time-of-day. The experimental values for two days in June agreed closely with the values computed using the above equations (Figure 10). During both days the mornings were clear, but increasing cloudiness occurred in the afternoon.

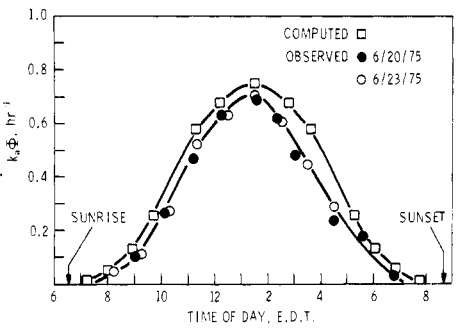

Figure 10. Time-of-day dependence of direct photolysis of DMDE at Athens, Ga.

Experimental midday half-lives for the direct photolysis of DMDE from spring to winter during 1975 agreed reasonably well with computed values (Figure 11). The rapid increase in half-life during November and December is attributed to the sharp decline in UV-B intensity during this period.

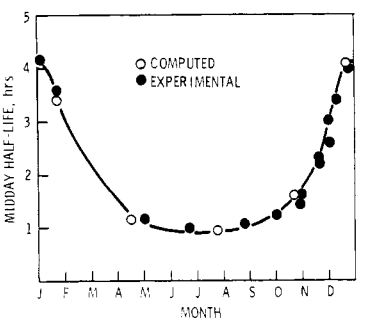

Figure 11. Seasonal variation of direct photolysis of DMDE at Athens, Ga., during 1975

Computed half-lives were in reasonable agreement with the experimental values for photolysis of pesticides and pesticide derivatives ranging in half-life from 3 min to 168 h (Figure 12). Generally, the computed half-lives were within ±30% of the experimental values.

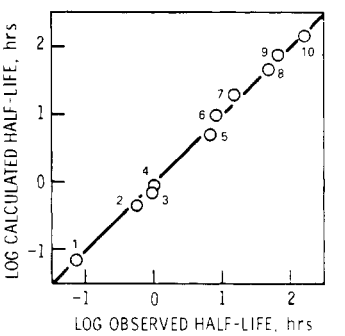

Figure 12. Comparison of calculated and observed half-lives for direct photolysis of several pesticides and pesticide derivatives (quantum yields parenthesized)

1, *N*-nitrosoatrazine in water (ϕ = 0.30); 2, trifluralin in water (ϕ = 0.0020); 3, DMDE in water (ϕ = 0.30); 4, DMDE in hexadecane (ϕ = 0.20); 5, DDE in hexadecane (ϕ = 0.26); 6, diphenylmercury in water (ϕ = 0.27); 7, phenylmercuric acetate in water (ϕ = 0.25); 8, 2,4-D-butoxyethyl ester in hexadecane (ϕ = 0.17); 9, carbaryl in water (ϕ = 0.0060); 10, 2,4-D-butoxyethyl ester in water (ϕ = 0.056)

Conclusions

The technique described above provides a simple method for computing direct photolysis rates of aquatic pollutants. The rates are computed from reproducible, readily obtainable data, the quantum yield for reaction and the electronic absorption spectrum of the pollutant. Even in the absence of quantum yield data, the mininum photolysis half-life and its variation with season, latitude, time-of-day, and depth can be computed from the absorption spectrum (Equation 15).

Some limitations of the computations are discussed below.

- Exposure to the sun and whole sky at sea level is assumed. Clouds reduce the UV-B intensity about 50% under overcast conditions (*2, 10, 15*). Intensity increases about 15–20% per kilometer increase in elevation (*11*).
- Daily variations in atmospheric ozone amount can be as high as 30% at midlatitudes (*30*). These variations can cause deviations from the computed rates, since they are based upon average ozone amounts (Figure 8). Pollutants that absorb sunlight most strongly at wavelengths >320 nm are little affected by ozone variation.
- The computations assume that the natural organics in a water body act only as photochemically inert "sunscreens". This assumption is valid only with respect to the direct photolysis process. Recent studies have shown that these natural substances are not photochemically inert, but may act as "sensitizers" that cause other photochemical processes to occur (*3, 4, 6, 33*).
- The effects of light scattering in water bodies are ignored. Scattering is likely to have an important effect upon the computed depth dependence in turbid lakes and rivers (*23*).
- In computing the average photolysis rate at a given depth, we have assumed that the pollutant is isotropically distributed and that all the pollutant in the water layer is exposed to the same amount of light during a given period of time. The latter assumption is always valid at depths in which only a small fraction of the incident light is absorbed (up to several meters in clear lakes and the ocean). However, if at the depth considered, all of the light is absorbed in the upper part of the water column, the assumptions are valid only if mixing is more rapid than entry of the pollutant into the upper layer of the water body through industrial discharge, atmospheric fallout, etc.; or loss of the pollutant from the upper layer through photolysis, vaporization, and other processes. If entry to the upper layer is more rapid than mixing, then the pollutant concentration will be highest near the surface. There is some evidence that this is the case in deep water bodies. For example, the concentration of CCl_3F, a chemically inert substance, declines with increasing depth in the ocean (*34*). On the other hand, Hedlund and Youngson have shown that lack of complete mixing can slow photolysis when the pollutant is, initially, uniformly distributed in the water column (*31*).

Despite the above limitations, our experiments at shallow depths have indicated that the computed rates are very close to those in the photic zone, which is usually well mixed. The computed rates should be a useful tool in evaluating the behavior of pollutants in the aquatic environment.

Acknowledgment

We thank Frank Lether and Donald Burkhard of the University of Georgia for their helpful discussions of the equations in this paper, G. L. Baughman and N. L. Wolfe of this laboratory for their help with certain derivations, and R. C. Fincher and J. A. Gordon for their technical assistance.

Literature Cited

(1) Altschuller, A. P., Bufalini, J. J., *Environ. Sci. Technol.*, **5,** 39 (1971).
(2) Leighton, P. A., "Photochemistry of Air Pollution", pp 6–41, Academic Press, New York, N.Y., 1961.
(3) Ross, R. D., Crosby, D. G., *J. Agric. Food Chem.*, **21,** 335 (1973).
(4) Ross, R. D., PhD dissertation, University of California, Davis, Calif., 1974.
(5) Zepp, R. G., Wolfe, N. L., Baughman, G. L., 168th Meeting, ACS, Atlantic City, N.J., September 1974.
(6) Zepp, R. G., Wolfe, N. L., Gordon, J. A., Baughman, G. L., *Environ. Sci. Technol.*, **9,** 1144 (1975).
(7) Hulburt, E. O., *J. Opt. Soc. Am.*, **35,** 698 (1945).
(8) Dawson, L. H., Hulburt, E. O., *ibid.*, **24,** 175 (1934).
(9) London, J., *Beitr. Phys. Atmos.*, **34,** 254 (1963).
(10) Green, A.E.S., Sawada, T., Shettle, E. P., *Photochem. Photobiol.*, **19,** 251 (1974).
(11) Bener, P., "Approximate Values of Intensity of Natural Ultraviolet Radiation for Different Amounts of Atmospheric Ozone", U.S. Army Report DAJA37-68-C-1017, Davos Platz, Switzerland, 1972.
(12) Johnson, F. S., *J. Meteorol.*, **11,** 431 (1954).
(13) Inn, E.C.Y., Tanaka, Y., *J. Opt. Soc. Am.*, **43,** 870 (1953).
(14) Koller, L. R., "Ultraviolet Radiation", Wiley, New York, N.Y., 1965.
(15) Urbach, F., Ed., "The Biologic Effects of Ultraviolet Radiation", pp 329–443, Pergamon Press, New York, N.Y., 1969.
(16) Grobecker, A. J., Coroniti, S. C., Cannon, R. H., "Report of Findings: The Effect of Stratospheric Pollution by Aircraft", U.S. Dept. of Transportation Report DOT-TST-75-50, Washington, D.C., December 1974.
(17) Zepp, R. G., Cline, D. M., unpublished results.
(18) International Critical Tables, Vol VII, p 13, McGraw-Hill, New York, N.Y., 1930.
(19) Hutchinson, G. E., "A Treatise on Limnology", Vol I, pp 366–423, Wiley, New York, N.Y., 1957.
(20) Poole, H. H., Atkins, W.R.G., *J. Mar. Biol. Assoc. UK*, **14,** 177 (1926).
(21) Whitney, L. V., *J. Opt. Soc. Am.*, **31,** 714 (1941).
(22) Lauscher, F., *Arch. Hydrobiol.*, **37,** 583 (1941).
(23) Tyler, J. E., Preisendorfer, R. W., in "The Sea", Vol 1, pp 397–451, M. N. Hill, Ed., Interscience, New York, N.Y., 1966.
(24) Duntley, S. Q., *J. Opt. Soc. Am.*, **53,** 214 (1963).
(25) Balzani, V., Carassiti, V., "Photochemistry of Coordination Compounds", pp 6–14, Academic Press, New York, N.Y., 1970.
(26) Calvert, J. G., Pitts, J. N., "Photochemistry", pp 686–814, Wiley, New York, N.Y., 1966.
(27) Moses, F. G., Liu, R.S.H., Monroe, B. M., *Mol. Photochem.*, **1,** 245 (1969).
(28) Turro, N. J., "Molecular Photochemistry", pp 18–19, Benjamin, New York, N.Y., 1965.
(29) Zepp, R. G., Wolfe, N. L., Fincher, R. C., unpublished results.
(30) Hammond, A. L., Maugh, T. H., *Science*, **186,** 335 (1974).
(31) Hedlund, R. T., Youngson, C. R., in "Fate of Organic Pesticides in the Aquatic Environment", S. Faust, Ed., pp 159–72, Advances in Chemistry Series, No. 111, American Chemical Society, Washington, D.C., 1972.
(32) Baughman, G. L., Gordon, J. A., Wolfe, N. L., Zepp, R. G., "Chemistry of Organomercurials in Aquatic Systems", U.S. EPA Report, EPA-660/3-73-012, September 1973.
(33) Zepp, R. G., Wolfe, N. L., Gordon, J. A., Fincher, R. C., *J. Agric. Food Chem.*, **24,** 727 (1976).
(34) Lovelock, J. E., Maggs, R. J., Wade, R. J., *Nature*, **241,** 194 (1973).

Received for review May 6, 1976. Accepted October 5, 1976.